International Journal of Pharmaceutics 373 (2009) 165–173

Contents lists available at ScienceDirect

International Journal of Pharmaceutics

journal homepage: www.elsevier.com/locate/ijpharm

Pharmaceutical Nanotechnology

Hyaluronic acid coated poly(butyl cyanoacrylate) nanoparticles as anticancer drug carriers

Miao He[a,b], Ziming Zhao[a,b], Lichen Yin[a], Cui Tang[a], Chunhua Yin[a,b,*]

[a] State Key Laboratory of Genetic Engineering, Department of Pharmaceutical Sciences, School of Life Sciences, Fudan University, Shanghai 200433, China
[b] Department of Biochemistry, School of Life Sciences, Fudan University, Shanghai 200433, China

ARTICLE INFO

Article history:
Received 15 October 2008
Received in revised form 17 January 2009
Accepted 12 February 2009
Available online 24 February 2009

Keywords:
Hyaluronic acid
Poly(butyl cyanoacrylate)
Nanoparticles
Paclitaxel
Drug delivery
Antitumor effect

ABSTRACT

The hyaluronic acid (HA) coated poly(butyl cyanoacrylate) (PBCA) nanoparticles were synthesized through radical polymerization of butyl cyanoarylate (BCA) initiated by cerium ions in the presence of HA. The chemical coupling between HA and PBCA was demonstrated by FTIR, ^{1}H NMR and X-ray diffraction. The sizes of the nanoparticles with different HA/BCA ratios were 291–325 nm at cerium concentration of 0.8 mmol/L and HA molecular weight of 18,000 Da. Paclitaxel (PTX), a model anticancer drug, was encapsulated in negatively charged nanoparticles with a maximal encapsulation efficiency of 90%. In vitro release demonstrated that HA modification could effectively reduce the initial burst release in the first 10 h and provide a sustained release in the subsequent 188 h. As evidenced by the hemolysis assay and MTT assay, HA coating could significantly reduce the cytotoxicity. Cellular uptake indicated that uptake of HA-PBCA nanoparticles by Sarcoma-180 (S-180) cells was 9.5-fold higher than that of PBCA nanoparticles. PTX-loaded HA-PBCA nanoparticles were more potent in tumor growth suppression than PTX-loaded PBCA nanoparticles or PTX injection following intravenous administration to S-180 tumor bearing mice. Therefore, the HA-PBCA nanoparticles could be an effective and safe vehicle for systemic administration of hydrophobic anticancer drugs.

1. Introduction

Nanoparticles have been studied as vehicles for antitumor drugs due to their small size, prolonged in vivo circulation and sustained drug release. It has been demonstrated that the surface property of nanoparticles is the key factor in modulating their biodistribution parameters (Lourenco et al., 1996; Peracchia et al., 1998). Nanoparticles with more hydrophobic surfaces will be preferentially taken up by the liver, and subsequently by the spleen and lung (Brigger et al., 2002). Plasma proteins and complement activation play a major role in the recognition of the particles by macrophages of the mononuclear phagocytes system (MPS) and in their rapid clearance from the bloodstream. In comparison, hydrophilic polymers can create a cloud of chains at the particle surface that will repel plasma proteins. Thus, the surfaces of nanoparticles with hydrophilic modification are designed in order to reduce the opsonization.

Poly(alkylcyanoacrylate) as drug carriers have been investigated extensively for nearly 30 years due to their low toxicity and biodegradability. Poly(alkylcyanoacrylate) nanoparticles were firstly developed through anionic emulsion polymerization by Couvreur et al. (1979). However, the nanoparticles obtained were rapidly cleared from the bloodstream by macrophage uptake. To prevent this uptake it has been suggested to modify the surface with more hydrophilic polymers. The most popular approach is grafting poly(ethylene glycol) (PEG) chains at the particle surface. The tissue distribution of PEG-coated poly(alkylcyanoacrylate) nanoparticles mainly depend on the different microvascular permeability between healthy tissues and tumors as well as their long circulating properties (Bazile et al., 1995; Chauvierre et al., 2003a). Another approach is coating nanoparticles with polysaccharides that have specific receptors in certain cells or tissues, thus achieving active targeting (Lemarchand et al., 2006). Some of the polysaccharides also have biological activity. For example, heparin has been used to prepare anticancer carrier due to its antiproliferative effect on tumor and endothelial cells (Park et al., 2006). Therefore, polysaccharide coated nanoparticles could be a new tendency in drug delivery systems. Chauvierre et al. (2003a) prepared polysaccharide modified poly(isobutyl cyanoacrylate) nanoparticles that preserved the biologic activity of the polysaccharide. The properties of nanoparticles depended on the polysaccharide. However, hyaluronic acid (HA), chitosan, and pectin formed microparticles with diameters from 30 to 59 μm which limited their application in drug delivery system due to the large particle size.

* Corresponding author at: State Key Laboratory of Genetic Engineering, School of Life Sciences, Fudan University, Shanghai 200433, China. Tel.: +86 21 6564 3797; fax: +86 21 5552 2771.
E-mail address: chyin@fudan.edu.cn (C. Yin).

0378-5173/$ – see front matter © 2009 Elsevier B.V. All rights reserved.
doi:10.1016/j.ijpharm.2009.02.012

HA is a linear, negatively charged polysaccharide, consisting of two alternating units of D-glucuronic acid and N-acetyl-D-glucosamine. As a major component of extracellular matrix in connective tissues, vitreous, and synovial fluids, it plays a critical role in cell growth, differentiation, migration, wound healing, and even cancer metastasis (Entwistle et al., 1996). HA has been used to prepare microspheres as gene delivery vehicle (Yun et al., 2004). Besides, HA-binding receptors CD44 (Day and Prestwich, 2002) and RHAMM (Yang et al., 1993) are over-expressed in various tumors. The HA level is elevated in cancer cells (Toole et al., 2002), forming a less dense matrix and leading to the enhanced cell motility and invasive ability into healthy tissues. Because of its high tumor specificity and biocompatibility, HA could be potentially used for the design of tumor-targeting drug delivery vehicles for anticancer drugs such as paclitaxel (PTX).

In the present study, HA coated poly(butyl cyanoacrylate) (PBCA) nanoparticles were prepared as an anticancer drug delivery vehicle through radical emulsion polymerization of n-butyl cyanoacrylate (BCA) monomers initiated by cerium ions in the presence of HA. The nanoparticles were characterized by FTIR, ^{1}H NMR, X-ray diffraction, photon correlation spectroscopy (PCS), zeta potential analysis, and transmission electron microscopy (TEM). With PTX as a model anticancer drug, the encapsulation efficiencies of the nanoparticles and in vitro drug release behavior were investigated. The biocompatibility of the nanoparticles was estimated in terms of hemolysis and MTT assay. The Sarcoma-180 (S-180) cellular uptake of PBCA and HA coated PBCA nanoparticles were determined. Finally, the anticancer efficiency of PTX-loaded nanoparticles was investigated in S-180 bearing mice.

2. Materials and methods

2.1. Materials

HA (MW18, 100, 500 and 1000 kDa) were obtained from Zhenjiang Dong Yuan Biotech Company Limited (Jiangsu, China). BCA monomers were obtained from Suncon Medical Adhesive Company (Beijing, China). Acetonitrile (Merck, Germany) was of HPLC grade. All the other reagents were of analytical grade.

Male KM mice weighing 18–22 g were provided by the Animal Care Center, Fudan University. Male New Zealand rabbits weighing 2.0–2.5 kg were provided by the Animal Care Center, Second Military Medical University.

S-180 cells and HEK-293 cells were purchased from the Institute of Biochemistry and Cell Biology, Shanghai Institutes for Biological Sciences, Chinese Academy of Sciences (Shanghai, China). S-180 cells were cultured in RPMI-1640 medium (Gibco, USA), supplemented with 10% (v/v) heat-inactivated fetal calf serum (FCS), 2 mmol/L glutamine, and 0.1 mg/mL of both penicillin and streptomycin. HEK-293 cells were cultured in Dulbecco's modified Eagle medium (Gibco, USA). Cells were cultured in a humidified atmosphere of 5% CO_2 at 37 °C.

Animal study protocol was reviewed and approved by the Institutional Animal Care and Use Committee, Fudan University, China.

2.2. Preparation and characterization of HA-PBCA nanoparticles

2.2.1. Preparation of HA-PBCA nanoparticles

HA-PBCA nanoparticles were prepared by radical polymerization of HA and BCA monomers. Briefly, HA was dissolved in 9 mL of nitric acid (0.2 mol/L) under gentle stirring and nitrogen gas bubbling. Ten minutes later, a solution of cerium ammonium nitrate was added, followed by addition of BCA monomers mixed with 1 mL of nitric acid under vigorous agitation. The pH of the polymerization system was maintained at around 0.7. The reaction was terminated after 3 h. The obtained nanoparticle suspensions were dialyzed against water for 48 h (molecular weight cut-off of 3500 Da). To study the influence of the reaction conditions on the characteristics of nanoparticles, various HA/BCA ratios (1:1–1:6 (w/w)), cerium ammonium nitrate concentrations (0.4–1.4 mmol/L), and HA molecular weight were used.

Unmodified nanoparticles were prepared as follows. Briefly, 50 μL of BCA monomers were dispersed in 5 mL of pH 2.5 HCl solution containing 0.5% poloxamer 188 as stabilizer and were allowed to polymerize spontaneously for 4 h under vigorous stirring. The obtained nanoparticle suspensions were dialyzed against water for 48 h (molecular weight cut-off of 3500 Da).

2.2.2. Characterization of HA-PBCA nanoparticles

Infrared spectra of HA and lyophilized HA-PBCA nanoparticles were obtained using a Thermo Nicolet Nexus 470 FTIR spectrometer (USA).

The lyophilized HA-PBCA nanoparticles were dissolved in a mixed solvent of 0.5 mL of DMSO-d_6 (99.9 atom% deuterium, Cambridge Isotope Laboratories, Inc.) and 100 μL of trifluoroacetic acid-D (99.5 atom% deuterium, Cambridge Isotope Laboratories, Inc.). The internal reference was tetramethylsilane (TMS). ^{1}H NMR spectrum was recorded with a Bruker AVANCE DMX 500 spectrometer (Germany).

X-ray diffraction spectra were obtained using a D/max-γB multicrystal diffraction meter (Rigaku, Japan) with CuKα radiation in the range of 2.5–50°(2θ) at 40 kV and 60 mA.

2.3. Particle size measurement

The particle size of the nanoparticles was measured by photon correlation spectroscopy with a Zeta Potential/Particle Sizer (Nicomp^{TM}380 ZLS, USA). All measurements were done at a wavelength of 635 nm at 23 °C with an angle detection of 90°. The particle size was expressed by mean effective diameter.

2.4. Surface charge

Zeta potential of the nanoparticles was measured on PCS (Nicomp^{TM}380 ZLS, USA). Each sample was measured three times at 23 °C.

2.5. Morphology

Nanoparticle suspensions were mounted on a Formvar-coated copper grid and subjected to negative staining with sodium phosphotungstate solution (0.2%, w/v). After 3 min of incubation at room temperature, the grid was air-dried and the morphology of the nanoparticles was visualized using a TEM (H-600A, Hitachi, Japan).

2.6. Preparation and characterization of PTX-loaded HA-PBCA nanoparticles

2.6.1. Preparation of PTX-loaded HA-PBCA nanoparticles

PTX in ethanol was slowly added to HA-PBCA nanoparticle suspensions under stirring. The resulting suspensions were sonicated for 240 s at 60 W output, dialyzed against water to remove residual ethanol and filtered through 0.80 μm membrane to remove PTX precipitates.

2.6.2. Encapsulation efficiency

Silica gel column (1.5 cm × 15 cm) was equilibrated with saline, and the PTX-loaded nanoparticle suspensions were loaded. The column was eluted with saline at a flow rate of 1.0 mL/min in order to separate nanoparticles from free PTX solubilized in nanoparticle suspensions. Different gradient of ethanol solutions were then used

to elute free PTX. The nanoparticle fraction was collected, and the volume (V) was measured. Elution was monitored at 280 nm using a UV-WXJ 9388 spectrophotometer.

The eluted nanoparticle fraction was dissolved in methanol and centrifuged at 12,000 rpm for 10 min to extract encapsulated PTX. The supernatant was filtered through 0.45 μm membrane, and the concentration (C) of PTX was determined by high performance liquid chromatography (HPLC). The HPLC apparatus was equipped with a Simadzu LC-10AD pump, a UV detector (Simadzu, SPD-10VP) operated at a wavelength of 227 nm. The column used was Hypersil C18 column (5 μm, 150 mm × 4.6 mm, Yilite, China). The mobile phase was acetonitrile/water (46/54, v/v) and the flow rate was 1.0 mL/min. The mass of PTX encapsulated in the nanoparticles was calculated as $C \times V$. The encapsulation efficiency (EE) was defined as follows.

$$\text{EE (\%, w/w)} = \text{Mass of drug encapsulated in nanoparticles} \times 100/\text{Mass of feed drug}$$

2.6.3. In vitro drug release

In vitro release of PTX was investigated using a dialysis method in phosphate buffered saline (PBS, pH 7.4) containing 0.1% (w/v) tween 80. Briefly, 1 mL of PTX-loaded nanoparticle suspensions were placed in a dialysis bag (molecular weight cut-off of 14 kDa) and dialyzed against 30 mL of the release medium at 100 rpm under 37 °C. At predetermined time intervals, the entire medium was removed and replaced with the same amount of fresh release medium. Following filtration through 0.45 μm membrane, the amount of PTX released was determined using HPLC.

2.7. Biocompatibility of nanoparticles

2.7.1. Hemolysis

Erythrocytes were isolated from whole blood of healthy New Zealand rabbit, washed three times with saline and resuspended to obtain a concentration of 2% (v/v). Saline was added into nanoparticle suspensions (0.1 and 0.2 mL) to obtain a final volume of 2.5 mL, into which 2.5 mL of erythrocyte suspension was added. The final concentrations of nanoparticles were 0.1 and 0.2 mg/mL. Samples were incubated at 100 rpm under 37 °C for 1 h, and then centrifuged at 3000 rpm for 10 min. The supernatant was analyzed for hemoglobin content at 541 nm using spectrophotometry. Erythrocytes incubated with saline and water served as negative and positive controls, respectively. Hemolysis ratio (HR) was calculated from the following equation.

$$\text{HR (\%)} = (\text{OD}_{541} \text{ of sample} - \text{OD}_{541} \text{ of negative control}) \times 100/(\text{OD541 of positive control} - \text{OD}_{541} \text{ of negative control})$$

2.7.2. Cytotoxicity

HEK-293 cells were seeded in 96-well plates at a density of 1×10^4 cells/well in Dulbecco's modified Eagle medium and subsequently cultured in a humidified atmosphere of 5% CO_2 at 37 °C for 24 h. HA-PBCA and PBCA nanoparticles at concentrations of 5.0, 1.0, and 0.2 mg/mL were added, respectively. Four hours later, the medium was removed and the cells were washed with PBS. The cell viability was quantitatively analyzed by the MTT assay.

2.8. Cellular uptake

Pyrene was encapsulated in nanoparticles as a probe for the uptake study. Pyrene loaded nanoparticles were prepared by incorporating pyrene instead of PTX in the nanoparticles as described in Section 2.6.1. The suspension was centrifuged at 3000 rpm for 10 min, and the supernatant was filtered through 0.8 μm membrane to remove the free pyrene which would precipitate in the aqueous environment.

Pyrene-loaded PBCA or HA-PBCA nanoparticles were added into S-180 cells, and incubated for 2 h at 37 °C, respectively. The cells were collected by centrifugation and washed three times with PBS, and then lysed with DMF. Pyrene that was encapsulated in the nanoparticles would be completely dissolved. The amount of pyrene in the cell lysis was quantified using spectrofluorimetry (Cary Eclipse, Varian, USA) (pyrene, λ_{ex} = 334 nm, λ_{em} = 394 nm), which correlated to the uptake amount of nanoparticles. Protein content of the cell lysis was measured by the Lowry method. The uptake of nanoparticles was calculated as the amount of pyrene per microgram of protein.

2.9. Antitumor effect

Two hundred microliter of S-180 cell suspension (1×10^6 cells) was inoculated subcutaneously to KM mice at the axillary region. It took 4–5 days for the tumor to reach 100 mm^3. Then, the tumor bearing mice were allocated to four groups for following treatment: (i) saline (control group); (ii) PTX injection (6 mg/kg PTX eq.); (iii) PTX-loaded PBCA nanoparticles (6 mg/kg PTX eq.); and (iv) PTX-loaded HA-PBCA nanoparticles (6 mg/kg PTX eq.). The drugs were administered 3 times in the first 5 days through intravenous injection, 1 day spaced between two administrations. The lengths of the longest tumor axis (L (t), mm) and the vertical axis (S (t), mm) were measured with a caliper every other day, and the tumor volume (V (t), mm^3) was calculated using the following equation.

$$V(\text{t}) = L(\text{t}) \times \frac{(S(\text{t}))^2}{2}$$

The mice were sacrificed on the 12th day after the first administration and the tumors were excised and weighed. The tumor inhibition ratio (TIR) was calculated using the following equation.

$$\text{TIR}(\%) = \left(\frac{1 - W(\text{t})}{W(\text{c})}\right) \times 100\%$$

where W (t) was the tumor weight of tested group and W (c) was the tumor weight of control group.

3. Results and discussion

3.1. Preparation of nanoparticles

Cerium ions were usually used as a highly efficient initiator in the redox radical polymerization in the presence of polysaccharides, which can lead to the cleavage of the polysaccharides in acidic medium and produce radicals at the end of chains, and thereby result in the polymerization of BCA monomers (Caner et al., 1998; Chauvierre et al., 2003a; Zhang et al., 2003; Krishnamoorthi et al., 2007). The main challenge of the synthesis procedure was to promote the redox radical polymerization by inhibiting the anionic spontaneous polymerization. Since BCA was a kind of highly reactive monomer which could polymerize spontaneously in emulsion after anionic initiation, the reaction was carried out at pH value lower than 1.0 to inhibit the anionic polymerization that occurred spontaneously due to the rapid initiation by the OH^- of water. After addition of Ce^{4+} and BCA monomers, an immediate and rapid increase in the turbidity of the reaction system was noted within 10 min, indicating that the reaction between HA and BCA was successfully initiated by Ce^{4+}. Comparatively, turbidity of the reaction system which was initiated by the hydroxyl groups of HA was not altered within 1 h in the absence of Ce^{4+} (data not

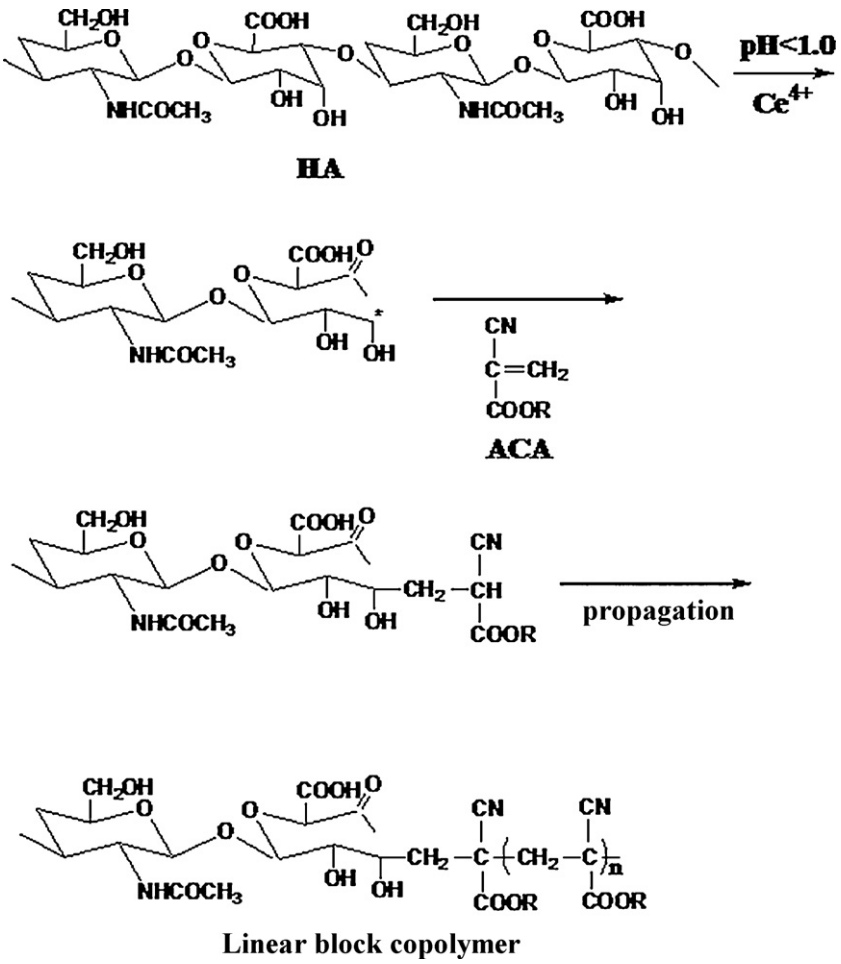

Fig. 1. Synthesis scheme of HA-PBCA nanoparticles prepared by redox radical polymerization.

shown). The hydroxyl groups were weak acids, it was unfavorable for their ionization at pH lower than 1.0. Therefore, it could be expected that the initiation of the polymerization induced by anion was strongly slowed down. Similar results were also obtained by previous investigations. Bertholon-Rajot et al. (2005) measured the diameter of the particles at different reaction times to determine the rate of anionic spontaneous polymerization and redox radical polymerization. Results suggested that the redox radical polymerization occurred much faster than anionic spontaneous polymerization initiated by the OH groups of dextran. The same phenomenon was found by Chauvierre et al. (2003a), who monitored the polymerization by turbidity measurements and reported that radical polymerization occurred faster than the anionic polymerization due to the high reactivity of the initiation step during the polymerization. Radicals were produced at the same time by the action of Ce^{4+} on the polysaccharides, initiating the polymerization as soon as the monomer was added into the medium. According to Chauvierre et al. (2003b), the process of polymerization was divided into three steps (Fig. 1). Firstly, radicals were created at a HA chain end by Ce^{4+} at the pH value lower than 1.0, bringing about simultaneous split of the HA chain. Then, BCA monomers were polymerized onto HA in the initiation of radicals. Finally, the polymerization propagated to a linear copolymer HA-PBCA with blocks of hydrophilic HA and hydrophobic PBCA, which exhibited amphiphilic property and could self-assemble into nanoparticles in water. The obtained nanoparticle suspensions were lyophilized and gravimetrically analyzed, which resulted in a yield of about 70%. The similar kinetic schemes were given by other researchers. Chitosan-poly(triethylene glycol dimethacrylate) was prepared by Yilmaz et al. (2007). The mechanism was that treatment of chitosan with Ce^{4+} resulted in oxidation and chain scission via radical formation. In the absence of monomers, radicals could lead to the formation of pyrone and pyranose rings. In the presence of monomers, radicals could initiate the polymerization of monomers onto the polysaccharides chains. In the present investigation, the hydrolytic degradation might occur when HA was dissolved in strong acid solution. However, such acidic hydrolysis would not significantly alter the subsequent polymerization mechanism as initiated by Ce^{4+}. Changes of the molecular weight of HA after being dissolved in strong acid need to be further studied.

3.2. Characterization of HA-PBCA nanoparticles

Fig. 2(A) showed the FTIR spectra of HA and HA-PBCA copolymers. The absorption bands at 3200–3600 cm^{-1} corresponded to the —OH group of HA. The bands at 2249 and 1752 cm^{-1} were respectively attributed to the —CN stretching vibration and the ester carbonyl of the PBCA, which verified the polymerization of BCA monomers onto HA chains.

The ^1H NMR spectra of HA and the copolymers with different HA/BCA ratios were shown in Fig. 2(B). The signals at A (1.98 ppm) and B (3.82–3.10 ppm) were attributed to the methyl protons in acetylamine groups and the protons in the sugar ring of HA, respectively. The broad peak at F (2.80–2.50 ppm) was attributed to the methylene protons of poly(cyanoacrylate). The peak at G (4.16 ppm) corresponded to the methylene in the α-position of the ester groups. Signals at C (0.92 ppm), D (1.42 ppm), and E (1.66 ppm) rep-

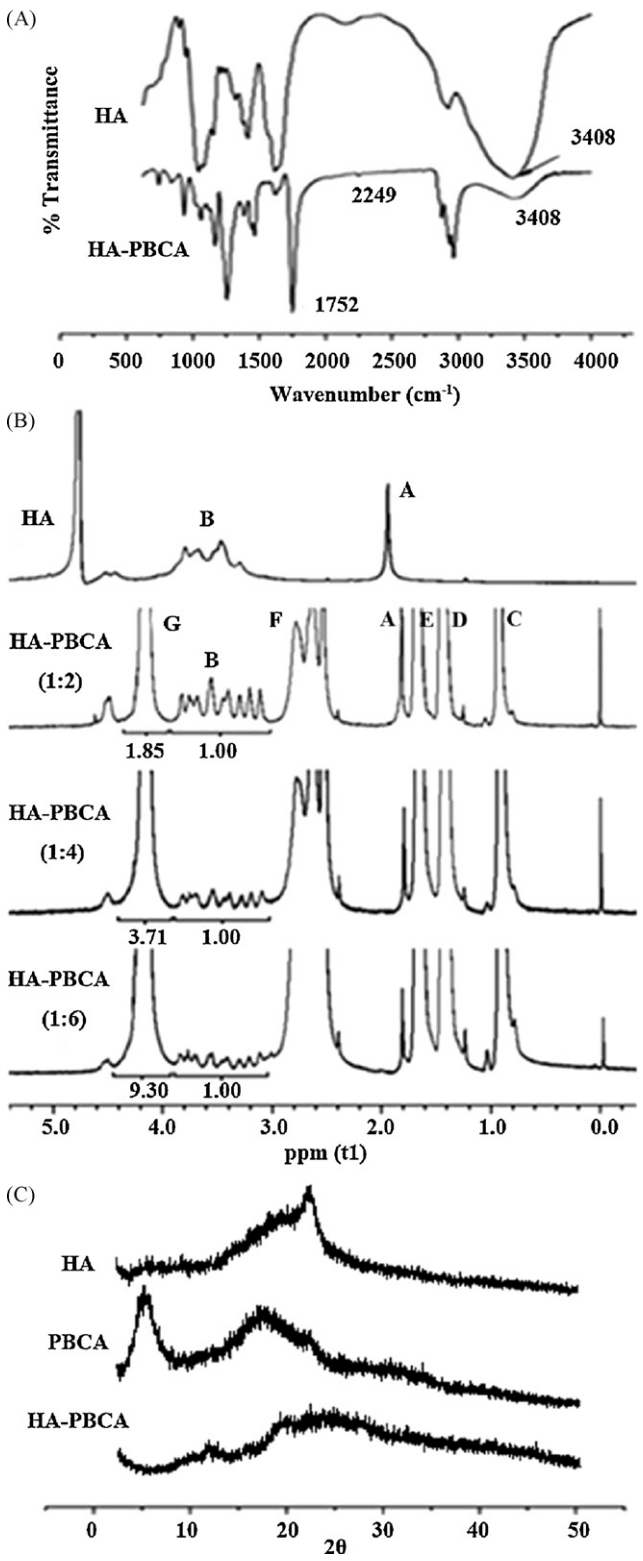

Fig. 2. (A) FTIR spectra of HA and HA-PBCA copolymer, (B) ^{1}H NMR spectra of HA in D_2O and HA-PBCA (1:2), HA-PBCA (1:4), HA-PBCA (1:6) in a mixed solvent of DMSO-d_6 and trifluoroacetic acid-D, and (C) X-ray diffraction spectra of HA, PBCA and HA-PBCA.

resented the methyl and methylene protons of the butyl chains. Based on the integral of signals at B and G, the molar ratios of disaccharide units of HA to BCA monomers were calculated to be about 1:12, 1:24, and 1:60, corresponding to the HA/BCA feed ratio (w/w) of 1:2, 1:4, and 1:6, respectively.

The X-ray diffraction spectra of HA, PBCA and HA-PBCA were shown in Fig. 2(C). HA contained two diffraction peaks at around $2\theta = 20.0^\circ$ and $2\theta = 22.5^\circ$, the peak at $2\theta = 22.5^\circ$ was relatively sharper. While, PBCA consisted of two major peaks at around $2\theta = 6.0^\circ$ and $2\theta = 17.5^\circ$. As for HA-PBCA, the sharp peaks at $2\theta = 22.5^\circ$ appeared in HA and the distinct peak at $2\theta = 6.0^\circ$ and $2\theta = 17.5^\circ$ observed in PBCA decreased with the appearance of two broad peaks at around $2\theta = 12.5^\circ$ and $2\theta = 25.0^\circ$. The HA chain was a regular, left-handed 3-fold helix stabilized by O—O intramolecular hydrogen bonds across the two kinds of glycosidic linkage (Winter et al., 1975). It was suggested that the polymerization of BCA onto HA chains led to the decrease of hydrogen bonding interaction of HA, and the crystalline structure of HA-PBCA appeared amorphous.

3.3. Particle size

3.3.1. Effect of HA/BCA ratio on particle size

Fig. 3(A) showed the effect of HA/BCA ratio on particle size. When HA/BCA ratio was 1:1, the particle size was larger than 400 nm and the turbidity of the suspensions was low, indicating that a few number of particles were formed. When the HA content was decreased, the particle size reduced from 432 to 291 nm. The hydrophilic HA was much expanded and swollen at the surface of the nanoparticles in water, which formed the shell. A decrease in the HA content with a constant concentration of cerium could produce more radicals and cleavages, thus yielding smaller fragments of hydrophilic HA chains. Besides, an increase in the content of BCA monomers favored formation of longer hydrophobic PBCA chains, which produced larger hydrophobic force and thereby resulted in a more compact hydrophobic core and smaller particles. When HA/BCA ratio was higher than 1:1, the obtained polymer molecules were water-soluble and it was even more difficult for them to form particles (data not shown).

3.3.2. Effect of initiator concentration on particle size

The concentration of cerium was another important parameter that influenced the particle size. It showed no significant effect on the effective diameter in the range of 0.4–0.8 mmol/L (Fig. 3(B)), which remained constant at about 325 nm. A further increase in the cerium concentration led to larger diameter. Theoretically, more radicals and cleavages should be created with the increased concentration of cerium, leading to smaller fragments of HA chain, producing copolymers with small molecular weight, and forming nanoparticles with small particle size. Such discrepancy of our results to the theoretical concept might be ascribed to the hydrophobic/hydrophilic balance that played an important role in the formation of nanoparticles (Bertholon-Rajot et al., 2005). With the HA part being hydrophilic and the PBCA part being hydrophobic, different concentrations of cerium may lead to copolymers with different hydrophobic/hydrophilic balance. More copolymer molecules may be required to form a single particle at higher cerium concentrations and larger particle size was therefore achieved (Langer et al., 1996).

3.3.3. Effect of HA molecular weight on particle size

The size of the nanoparticles was mainly dependent on the molecular weight of HA (Fig. 3(C)). The particle size varied from 291 to 1010 nm as the molecular weight of HA increased from 18 to 1000 kDa. The HA-PBCA copolymer possessed a linear diblock structure and HA was expected to adopt an end-on conformation at the surface giving hairy nanoparticles (Bertholon-Rajot et al., 2005). HA with higher molecular weight formed longer hydrophilic chain, which expanded in water and led to larger particles.

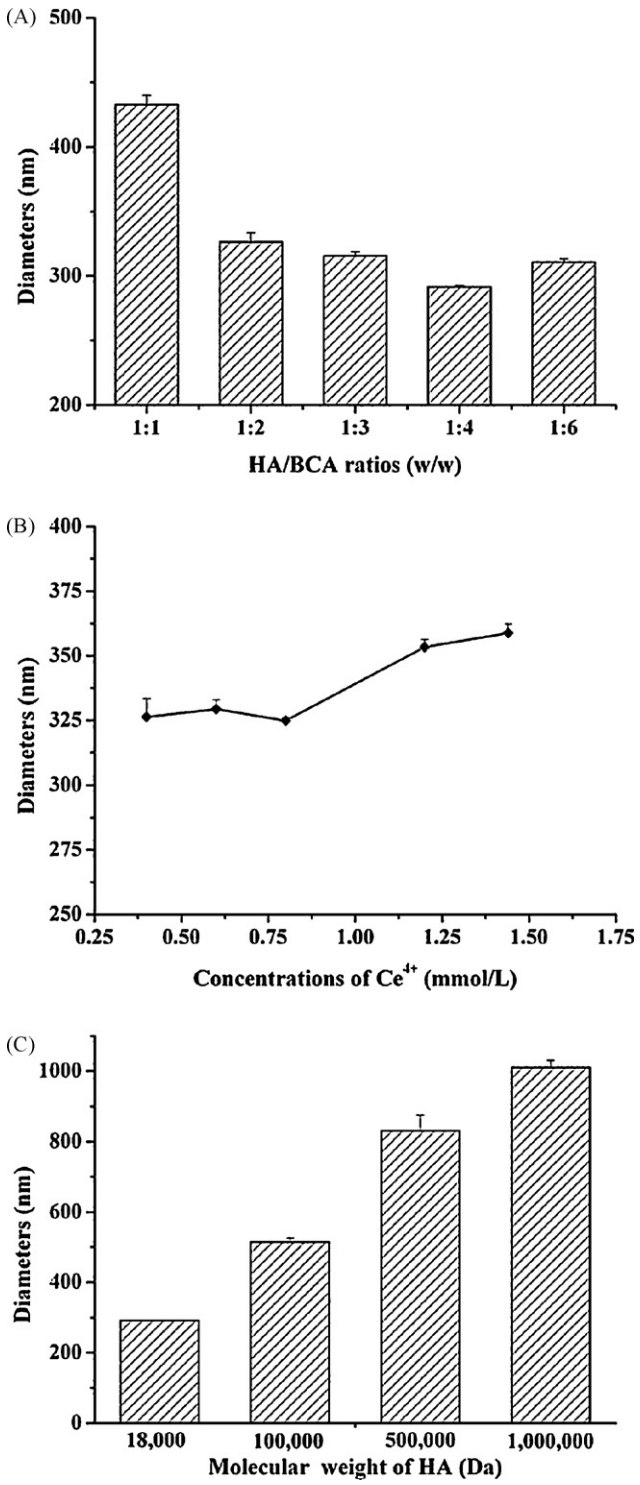

Fig. 3. Effect of several reaction conditions on particle size (mean ± SD, $n = 3$). The total concentration of HA and BCA monomer was 1.0% (w/v). (A) HA/BCA ratios (cerium concentration of 0.8 mmol/L and HA molecular weight of 18 kDa), (B) cerium concentrations (HA/BCA ratio 1:2 and HA molecular weight of 18 kDa), and (C) HA molecular weight (HA/BCA ratio 1:4 and cerium concentration of 0.8 mmol/L).

3.4. Surface charge

The zeta potential of nanoparticles with HA/BCA ratios of 1:1, 1:2, 1:3, 1:4, 1:6 were -35.58 ± 0.65, -32.58 ± 0.18, -42.26 ± 0.21, -42.95 ± 0.71, and -44.50 ± 0.63 mV, respectively, which confirmed that the HA/BCA ratio had inappreciable influence on the zeta potential. The zeta potential of the nanoparticles depended on the nature of the polysaccharide (Bertholon-Rajot et al., 2005). Since the carboxyl groups of HA were ionized and negatively charged at about pH 7.0, zeta potentials of the nanoparticles obtained were negative, correspondingly.

3.5. Morphological characterizations

TEM images of nanoparticles with HA/BCA ratio 1:2 were shown in Fig. 4. Nanoparticles appeared monodispersed spheres with a solid and consistent structure.

3.6. Encapsulation efficiency

Based on the results mentioned above, nanoparticles with HA/BCA ratios 1:2, 1:4, and 1:6, HA molecular weight of 18 kDa, and cerium concentration of 0.8 mmol/L were chosen for further studies, abbreviated as NP2, NP4, and NP6, respectively. The differences of the encapsulation efficiencies among variety nanoparticles were statistically analyzed using *t*-test. As shown in Fig. 5, the encapsulation efficiencies of the three kinds of nanoparticles were all over 85% when the concentration of PTX was 0.5 mg/mL, which demonstrated that HA-PBCA nanoparticles could be an effective vehicle for PTX. As the concentration of PTX increased from 0.5 to 1.0 mg/mL, the encapsulation efficiency decreased from 90.2 to 82.8% for NP2, 90.8 to 73.8% for NP4, and 85.6 to 71.7% for NP6, respectively. The encapsulation efficiency of NP2 was significantly higher than that of NP6 ($p < 0.05$). As compared with NP4 and NP6, NP2 possessed longer hydrophilic HA part and shorter hydrophobic PBCA part, leading to weaker hydrophobic interaction. During the sonication process, the hydrophobic cores of NP2 could disaggregate easily and reassemble again. Thus, more PTX could be incorporated into the hydrophobic part.

3.7. In vitro drug release

The in vitro release profiles of PTX from NP2, NP4, and NP6 were shown in Fig. 6. It exhibited an initial burst of 18.29 ± 1.24, 22.06 ± 3.00, and 21.09 ± 1.56% in the first 10 h, and an accumulative release of 50.02 ± 1.07, 51.75 ± 2.66, and 60.87 ± 3.23% after 188 h for NP2, NP4, and NP6, respectively. It could be noticed that a larger HA component in the nanoparticles corresponded to slower drug release and restriction in the initial burst. As the hydrophobic core of NP2 may possess strong affinity with PTX, it was difficult for PTX to release from the nanoparticles. Besides, the hydrophilic HA chains on the surface of NP2 were longer than those of NP4 and NP6, which may slow down the release of hydrophobic PTX.

3.8. Biocompatibility

3.8.1. Hemolysis

Hemolysis was an important factor in the evaluation of the biocompatibility of materials. Hemolysis ratio less than 5% was commonly regarded as nontoxic (Rao and Sharma, 1997). In the present investigation, hemolysis ratio of NP2, NP4, NP6 and PBCA at the final concentration of 0.1 mg/mL were 0, 0.37 ± 0.17, 1.69 ± 0.22, and 1.29 ± 0.05%, respectively ($n = 3$). When the final concentration was 0.2 mg/mL, the hemolysis ratio of NP2, NP4, NP6 and PBCA were 0.50 ± 0.16, 0.58 ± 0.03, 1.74 ± 0.22, and 2.02 ± 0.09%, respectively ($n = 3$). The hemolytic potential of all the HA-PBCA nanoparticles were below 2%, and a decrease in the HA content caused a slight increase in hemolysis ratio. The membrane of red blood cells (RBC) was soft and composed of two-sublayers, the outer sublayer being negatively charged and the inner one being positively charged. According to the study of Makino et al. (1999), the dominant factor to control the interaction between RBC and the synthetic polymer was the softness of the nanoparticle surface. It was considered that

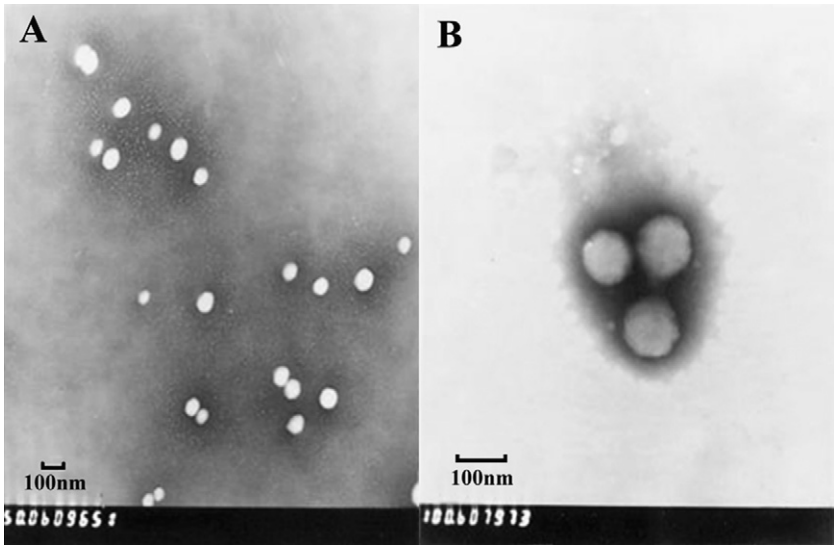

Fig. 4. TEM of nanoparticles prepared with HA/PBCA ratio 1:2, cerium concentration of 0.8 mmol/L, and HA molecular weight of 18 kDa. A: ×50,000 and B: ×100,000. Bar represents 100 nm.

synthetic polymers were not recognized as foreign materials by biological cells, if the polymer surfaces were soft and hydrophilic. The hydrophilic HA chains on the surface of the nanoparticles could prevent the rigid PBCA core from contacting the RBC, thus making the nanoparticles softer and decreasing the hemolytic potential.

3.8.2. Cytotoxicity

The results of MTT cytotoxicity assay were shown in Fig. 7. There was a significant increase ($p < 0.001$) in cell viability after exposure to NP2, NP4, and NP6 as compared to PBCA nanoparticle at the high concentrations of 5.0 and 1.0 mg/mL, indicating that the HA modification on the surface of PBCA nanoparticles could successfully decrease the cytotoxicity. There was no statistical difference ($p > 0.05$) in cytotoxicity between NP2 and the negative control when the concentrations were 1.0 and 0.2 mg/mL. HA-PBCA nanoparticles were primarily considered to exhibit minimal cytotoxicity when the concentration was below 1.0 mg/mL. Nanoparticles can cause cytotoxicity through adherence to the cell membrane, degradation of the adherent polymer, and subsequent release of cytotoxic degradation product (Müller et al., 1997). It was found that dextran coated poly(alkylcyanoacrylate) nanoparticles obtained by radical polymerization appeared 20-fold less cytotoxic than poly(alkylcyanoacrylate) nanoparticles obtained by anion emulsion polymerization. The polysaccharide chain con-

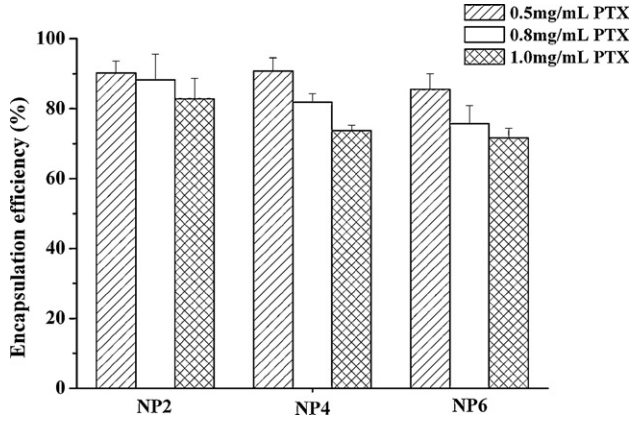

Fig. 5. Encapsulation efficiencies of HA-PBCA nanoparticles for PTX. The concentration of the three kinds of nanoparticles was fixed at 3.5 mg/mL (mean ± SD, $n = 3$).

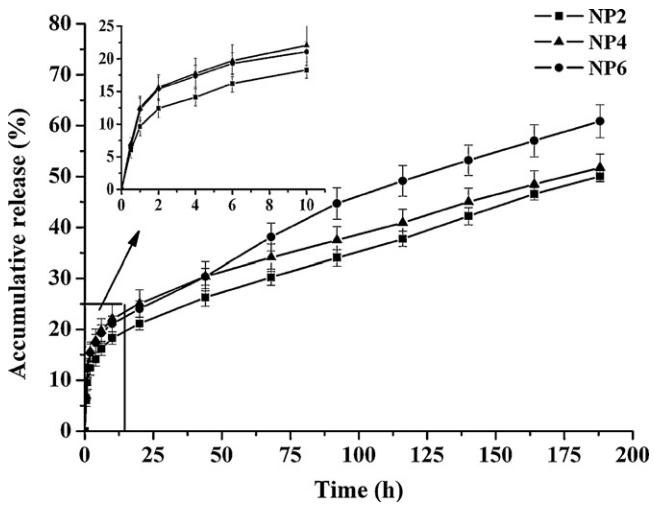

Fig. 6. In vitro drug release profiles of PTX from HA-PBCA nanoparticles in PBS (pH 7.4) containing 0.1% tween 80 (w/v) at 37 °C (mean ± SD, $n = 3$).

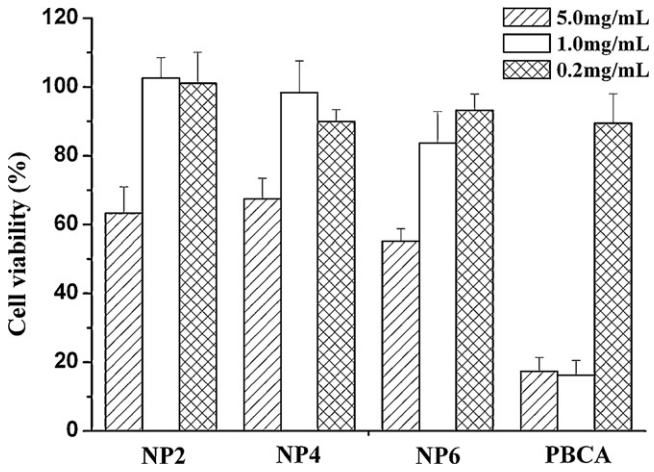

Fig. 7. Cell viability of HEK-293 cells incubated with HA-PBCA nanoparticles and PBCA nanoparticles (mean ± SD, $n = 5$).

formation at the nanoparticle surface may play a key role in modulating the interactions between nanoparticles and cells, hence modifying the cytotoxicity of the nanoparticles (Chauvierre et al., 2007). Therefore, the improvement of cell viability in HA-PBCA nanoparticles may be attributed to its hair-like conformation of the HA chain at the PBCA nanoparticle surface.

3.9. Cellular uptake

To ensure that the fluorescence intensity determined was due to the pyrene loaded nanoparticles, in vitro release of pyrene was firstly examined. The percentage of pyrene released from PBCA or HA-PBCA nanoparticles within 2 h was less than 10% (data not shown). Therefore, it could be assumed that the fluorescence intensity would be due to the pyrene loaded nanoparticles. The uptake of PBCA and HA-PBCA nanoparticles by S-180 cells in vitro were 0.21 ± 0.02 and 2.00 ± 0.24 nanogram pyrene per microgram protein, respectively, which demonstrated that uptake of HA-PBCA nanoparticles was 9.5-fold higher than unmodified nanoparticles ($p < 0.01$). According to the previous studies, various tumors cells over-expressed HA-binding receptors CD44 (Day and Prestwich, 2002) and RHAMM (Yang et al., 1993), as a result, the modification of HA at the nanoparticles' surface might increase its affinity towards S-180 cells, which would facilitate the targeting effect of PTX-loaded HA-PBCA nanoparticles to the tumor. Similar conclusion had been drawn by Jain and Jain (2008) in evaluation of uptake of HA coupled chitosan nanoparticles by HT-29 colon cancer cells.

3.10. Antitumor effect

S-180 was a classic tumor model which was selected by many researchers in antitumor efficiency evaluation. As the blood vessels were abundant around the tumors, the drugs could be transported to the tumors through blood circulation after systemic injection. Tumor model inoculated subcutaneously has its own merits. S-180 tumor grew subcutaneously at the axillary region, and therefore it was convenient to measure the tumor volume and investigate the tumor growth tendency. Moreover, it could also reflect the in vivo therapeutic effect of the drugs to some extent. NP2 was used for in vivo experiment. As shown in Fig. 8 and Table 1, all the three groups of PTX administration showed significant antitumor effects ($p < 0.01$) compared with the control group. In addition, the antitumor effects of PTX-loaded PBCA nanoparticles and PTX-loaded NP2 increased significantly than PTX injection group ($p < 0.001$). In particular, PTX-loaded NP2 turned out to be more efficient in tumor growth suppression than PTX-loaded PBCA nanoparticles ($p < 0.001$). Such superiority could be attributed to the following factors. Nanoparticles had been found to prolong the blood half-life of drugs and increase the efficacy of intravenous injection when compared to PTX injection which was rapidly eliminated (Williams et al., 2003). The hydrophilic HA chains on the surface of the nanoparticles were expanded and swollen in the water, which could create a cloud of chains at the particle surface and thereby might reduce opsonization by blood proteins and uptake by macrophages of the MPS. Therefore, it was speculated that PTX-loaded NP2 might circulate in the blood stream for longer periods than free PTX and increase the possibility of PTX-loaded NP2 accessing target sites. Besides, the result of cellular uptake showed that the HA-PBCA nanoparticles possessed stronger affinity towards S-180 cells than PBCA nanoparticles. With HA as a ligand to modify the nanoparticles, tumor-targeting effect could be achieved, leading to higher concentration of PTX-loaded nanoparticles in tumors. To verify such result, investigation on the tissue distribution of PTX in S-180 bearing mice is to be carried out in further studies.

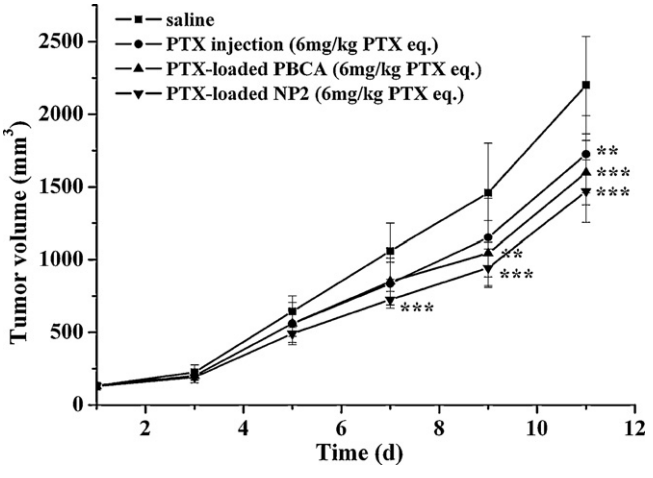

Fig. 8. Antitumor effect achieved in S-180 bearing mice following systemic administration of saline, PTX injection (6 mg/kg PTX eq.), PTX-loaded PBCA (6 mg/kg PTX eq.), and PTX-loaded NP2 (6 mg/kg PTX eq.) (mean ± SD, $n = 10$). Statistically significant difference from control: $^{**}p < 0.01$, $^{***}p < 0.001$.

Table 1
Tumor inhibition ratio (TIR) of PTX injection (6 mg/kg PTX eq.), PTX-loaded PBCA (6 mg/kg PTX eq.), and PTX-loaded NP2 (6 mg/kg PTX eq.) against S-180 tumor-bearing mice (mean ± SD, $n = 10$).

Drug	Tumor weight (g)	TIR (%)
Saline (control)	3.65 ± 0.79	–
PTX injection (6 mg/kg PTX eq.)	2.65 ± 0.28**	27.40
PTX-loaded PBCA (6 mg/kg PTX eq.)	1.89 ± 0.47***	48.22
PTX-loaded NP2 (6 mg/kg PTX eq.)	1.11 ± 0.20***	69.59

** Statistically significant difference from control: $p < 0.01$.
*** Statistically significant difference from control: $p < 0.001$.

4. Conclusion

The HA-PBCA nanoparticles were prepared by radical polymerization of HA and BCA monomers. The obtained nanoparticles were generally monodispersed spheres with a solid and consistent structure. The particle diameters could be influenced by HA/BCA ratio, cerium concentration, and HA molecular weight. The surface charges of the HA-PBCA nanoparticles were negative. High encapsulation efficiency of PTX was obtained and the maximal encapsulation efficiency was up to 90%. The in vitro release profiles showed that the modification of HA could slow down the drug release and reduce the initial burst in the first 10 h. The biocompatibility of HA-PBCA nanoparticles was desirable. Uptake of HA-PBCA nanoparticles by S-180 cells was significantly higher than unmodified nanoparticles. PTX-loaded HA-PBCA nanoparticles were more potent in tumor growth suppression than PTX-loaded PBCA nanoparticles or PTX injection. In conclusion, the HA-PBCA nanoparticles may be an effective and safe vehicle for hydrophobic anticancer drugs.

References

Bazile, D., Prud'homme, C., Bassoullet, M.-T., Marlard, M., Spenlehauer, G., Veillard, M., 1995. Stealth Me PEG-PLA nanoparticles avoid uptake by the mononuclear phagocytes system. J. Pharm. Sci. 84, 493–498.
Bertholon-Rajot, I., Labarre, D., Vauthier, C., 2005. Influence of the initiator system, cerium-polysaccharide, on the surface properties of poly(isobutylcyanoacrylate) nanoparticles. Polymer 46, 1407–1415.
Brigger, I., Dubernet, C., Couvreur, P., 2002. Nanoparticles in cancer therapy and diagnosis. Adv. Drug. Del. Rev. 54, 631–651.
Caner, H., Hasipoglu, H., Yilmaz, O., Yilmaz, E., 1998. Graft copolymerization of 4-vinylpyridine on to chitosan-1 By ceric ion initiation. Eur. Polym. J. 34, 493–497.
Chauvierre, C., Labarre, D., Couvreur, P., Vauthier, C., 2003a. Novel polysaccharide-decorated poly(isobutyl cyanoacrylate) nanoparticles. Pharm. Res. 20, 1786–1793.

Chauvierre, C., Labarre, D., Couvreur, P., Vauthier, C., 2003b. Radical emulsion polymerization of alkylcyanoacrylates initiated by the redox system dextran-cerium (IV) under acidic aqueous conditions. Macromolecules 36, 6018–6027.
Chauvierre, C., Leclerc, L., Labarre, D., Appel, M., Marden, M.C., Couvreur, P., Vauthier, C., 2007. Enhancing the tolerance of poly(isobutylcyanoacrylate) nanoparticles with a modular surface design. Int. J. Pharm. 338, 327–332.
Couvreur, P., Kante, B., Roland, M., Speiser, P., 1979. Absorption of anti-neoplastic drugs to polyalkylcyanoacrylate nanoparticles and their release in calf serum. J. Pharm. Sci. 68, 1521–1524.
Day, A.J., Prestwich, G.D., 2002. Hyaluronan-binding proteins: tying up the giant. J. Biol. Chem. 277, 4585–4588.
Entwistle, J., Hall, C.L., Turley, E.A., 1996. HA receptors: regulators of signalling to the cytoskeleton. J. Cell. Biochem. 61, 569–577.
Jain, A., Jain, S.K., 2008. In vitro and cell uptake studies for targeting of ligand anchored nanoparticles for colon tumors. Eur. J. Pharm. Sci. 35, 404–416.
Krishnamoorthi, S., Mal, D., Singh, R.P., 2007. Characterization of graft copolymer based on polyacrylamide and dextran. Carbohydr. Polym. 69, 371–377.
Langer, K., Marburger, C., Berthold, A., Kreuter, J., Stieneker, F., 1996. Methylmethacrylate sulfopropylmethacrylate copolymer nanoparticles for drug delivery Part I: preparation and physicochemical characterization. Int. J. Pharm. 137, 67–74.
Lemarchand, C., Gref, R., Passirani, C., Garcion, E., Petri, B., Müller, R., Costantini, D., Couvreur, P., 2006. Influence of polysaccharide coating on the interactions of nanoparticles with biological systems. Biomaterials 27, 108–118.
Lourenco, C., Teixeira, M., Simões, S., Gaspar, R., 1996. Steric stabilization of nanoparticles: size and surface properties. Int. J. Pharm. 138, 1–12.
Makino, K., Umetsu, M., Goto, Y., Nakayama, A., Suhara, T., Tsujii, J., Kikuchi, A., Ohshima, H., Sakurai, Y., Okano, T., 1999. Interaction between charged soft microcapsules and red blood cells: effects of PEGylation of microcapsule membranes upon their surface properties. Colloids Surf. B: Biointerfaces 13, 287–297.
Müller, R.H., Maassen, S., Schwarz, C., Mehnert, W., 1997. Solid lipid nanoparticles (SLN) as potential carrier for human use: interaction with human granulocytes. J. Control. Release 47, 261–269.
Park, K., Lee, G.Y., Kim, Y.-S., Yu, M., Park, R.-W., Kim, I.-S., Kim, S.Y., Byun, Y., 2006. Heparin-deoxycholic acid chemical conjugate as an anticancer drug carrier and its antitumor activity. J. Control. Release 114, 300–306.
Peracchia, M.T., Vauthier, C., Desmaële, D., Gulik, A., Dedieu, J.-D., Demoy, M., d'Angelo, J., Couvreur, P., 1998. Pegylated nanoparticles from a novel methoxypolyethylene glycol cyanoacrylate-hexadecyl cyanoacrylate amphiphilic copolymer. Pharm. Res. 15, 550–556.
Rao, S.B., Sharma, C.P., 1997. Use of chitosan as a biomaterial: studies on its safety and hemostatic potential. J. Biomed. Mater. Res. 34, 21–28.
Toole, B.P., Wight, T.N., Tammi, M.I., 2002. Hyaluronan–cell interactions in cancer and vascular disease. J. Biol. Chem. 277, 4593–4596.
Williams, J., Lansdown, R., Sweitzer, R., Romanowski, M., LaBell, R., Ramaswami, R., Unger, E., 2003. Nanoparticle drug delivery system for intravenous delivery of topoisomerase inhibitors. J. Control. Release 91, 167–172.
Winter, W.T., Smith, P.J.C., Struther, A., 1975. Hyaluronic acid: structure of a fully extended 3-fold helical sodium salt and comparison with the less extended 4-fold helical forms. J. Mol. Biol. 99, 219.
Yang, B., Zhang, L., Turley, E.A., 1993. Identification of two hyaluronan-binding domains in the hyaluronan receptor RHAMM. J. Biol. Chem. 268, 8617–8623.
Yilmaz, E., Adali, T., Yilmaz, O., Bengisu, M., 2007. Grafting of poly(triethylene glycol dimethacrylate) onto chitosan by ceric ion initiation. React. Funct. Polym. 67, 10–18.
Yun, Y.H., Goetz, D.J., Yellen, P., Chen, W., 2004. Hyaluronan micropheres for sustained gene delivery and site-specific targeting. Biomaterials 25, 147–157.
Zhang, J., Yuan, Y., Shen, J., Lin, S., 2003. Synthesis and characterization of chitosan grafted poly(N, N-dimethyl-N-methacryloxyethyl-N-(3-sulfopropyl ammonium)) initiated by ceric (IV) ion. Eur. Polym. J. 39, 847–850.